ELSEVIER

Deep-Sea Research II 51 (2004) 2841–2856

DEEP-SEA RESEARCH
PART II

www.elsevier.com/locate/dsr2

Iron enrichment and photoreduction of iron under UV and PAR in the presence of hydroxycarboxylic acid: implications for phytoplankton growth in the Southern Ocean

Murat Öztürk[a,*], Peter L. Croot[b,1], Stefan Bertilsson[c,2], Katarina Abrahamsson[d], Bengt Karlson[e,3], Roland David[f], Agneta Fransson[g,4], Egil Sakshaug[a]

[a]*Trondheim Biological Station, Norwegian University of Science and Technology, Bynesvägen 46, N-7018 Trondheim, Norway*
[b]*Department of Chemistry, Analytical and Marine Chemistry, Göteborg University, SE-412 96 Göteborg, Sweden*
[c]*Department of Water and Environmental Studies, Linköping University, SE-581 83 Linköping, Sweden*
[d]*Department of Chemistry and Bioscience, Chalmers University of Technology, SE-412 96 Göteborg, Sweden*
[e]*Botanical Institute, Göteborg University, Box 461, SE-405 30 Göteborg, Sweden*
[f]*CSIR, PO Box 17001, Congella 4013, Kwa-Zulu Natal, South Africa*
[g]*Department of Chemistry, Analytical and Marine Chemistry, Göteborg University, SE-412 96 Göteborg, Sweden*

Abstract

Iron(III) photoreduction and the responses of phytoplankton under ultraviolet (UV) and photosynthetically available radiation (PAR) were investigated with the presence of hydroxycarboxylic acid (glucaric acid (GA), a model compound for organic acids excreted by phytoplankton). The incubation experiments were carried out on board using seawater samples collected in the location of the winter ice edge (WIE) and the spring ice edge (SIE) of the Southern Ocean. In this paper, we focus on the results of experiment in WIE. Throughout the experiments, dissolved Fe(II), major nutrients and in vivo fluorescence were monitored regularly. In addition, Chl-*a*, POC/PON, cell densities of phytoplankton and bacteria, bacterial production, organic peroxide, hydrogen peroxide and total CO_2 were measured.

The results from the WIE show that iron enrichment had a substantial effect on phytoplankton growth rate. Fe(III) addition in the presence of GA (FeGA) gave higher Fe(II) concentration and higher growth rate of phytoplankton than those in controls. Our results suggest that hydroxycarboxylic acid had a significant chemical and biological impact. The presence of GA influenced iron photochemistry and iron availability to phytoplankton. Phytoplankton growth responses to iron enrichments in incubations under UV and PAR were completely dissimilar. It seems that FeGA

*Corresponding author. Tel.: +47 7359 1595; fax +47 7359 1597.
E-mail address: murato@bio.ntnu.no (M. Öztürk).
[1]Present address: Leibniz-Institut Marine Sciences at Kiel University (IFM-GEOMAR), Düsternbrooker Weg 20, D-24105 Kiel, Germany.
[2]Present address: Department of Evolutionary Biology/Limnology, Uppsala University, Norbyv. 20, SE-75236 Uppsala, Sweden.
[3]Present address: SMHI, Building 31, Nya Varvet, SE-426 71 Västra Frölunda, Sweden.
[4]Present address: Climate Change Research Project, National Institute for Environmental Studies, 16-2 Onogawa, Tsukuba, Ibaraki 305-8506, Japan.

0967-0645/$ - see front matter
doi:10.1016/j.dsr2.2000.10.001

addition prominently changes the harmful effect of UV on the phytoplankton population. This study provides preliminary information on how the photoreduction of iron(III) and the phytoplankton growth are affected by iron enrichment in the presence of hydroxycarboxylic acid.

1. Introduction

The Southern Ocean is distinguished by being far from the major terrestrial and anthropogenic sources of iron, and its cold surface waters are separated from other major oceans by the Antarctic Polar Front. Due to its remoteness from continents, iron concentrations are very low in the surface layers of the Southern Ocean (Löscher et al., 1997). Furthermore, the Southern Ocean is known to be an important area in the world's oceans in regulating the oceanic carbon cycle, thus playing a significant role in regulating atmospheric CO_2 (Bakker et al., 1997). Nitrate, phosphate and silicate concentrations in the Southern Ocean may reach above 30, 2.5 and 100 mmol m^{-3}, respectively (Sakshaug et al., 1991). In addition, the concentrations of chlorophyll *a* (Chl-*a*) and the standing stock of phytoplankton are low, on average 0.4 mg m^{-3} and <3 mg m^{-3} Chl-*a* in the ice-free and deep-sea regions of the Southern Ocean, respectively (El Sayed, 1988; Holm-Hansen et al., 1989). Hence, the Southern Ocean, as well as the equatorial Pacific, is a major high-nutrient and low-chlorophyll (HNLC) zone.

This HNLC situation may result in light limitation due to wind-induced deep mixing (Sakshaug and Holm-Hansen, 1984; Sakshaug et al., 1991) or iron limitation (Martin et al., 1990) and grazing control (Banse, 1990). Light and iron limitation may have a similar impact (Sakshaug et al., 1991), while grazing is always more or less important as a controlling factor at certain times and in different locations. These explanations are not mutually exclusive.

The importance of iron limitation of marine phytoplankton has become increasingly apparent in recent years. A breakthrough for the iron hypothesis was the in situ iron enrichment experiments with waters in the equatorial Pacific Ocean (IronEx I & II) (Martin et al., 1994; Behrenfeld et al., 1996; Coale et al., 1996). These mesoscale in situ Fe experiments showed that Fe is a limiting element in the equatorial Pacific Ocean. Fe enrichment stimulates phytoplankton production in the Southern Ocean (van Leeuwe et al., 1997; Scharek et al., 1997).

Iron can exist in two different oxidation states in seawater: Fe(III) and Fe(II). Fe(III) is thermodynamically stable in oxic waters. Fe(II) may be produced by photochemical reduction of Fe(III) in surface seawater (Miller and Kester, 1994a). It is believed that Fe(II) in seawater exists mainly as "free" Fe^{2+} ions and is much more soluble than Fe (III) (Stumm and Morgan, 1996). Therefore it may be effectively available for phytoplankton. However, it has been argued that Fe(II) in seawater oxidizes too rapidly with half life of a few minutes (Millero et al., 1987; Morel et al., 1991) to be important. Nevertheless, significant concentrations of Fe(II) have been observed in coastal waters (Kuma et al., 1992; Zhuang et al., 1995). Dissolved organic matter (DOM) such as humic acids and hydroxycarboxylic acids, which inpart is released by phytoplankton (Kuma et al., 1992, 1995), may play an important role in the photoreduction of Fe(III) by providing an electron source. Some DOM components can slow down the re-oxidation rate by complexation with Fe(II) (Hudson et al., 1992). However, it is not yet clear to what extent this is important in seawater. On the other hand, photochemically produced radicals, for example, $O_2^{\bullet -}$, H_2O_2, $HO_2^{\bullet\prime}$ and $OH^{\bullet}$, can participate in secondary oxidation and reduction of Fe species in seawater (Faust and Zepp, 1993; King et al., 1995; Voelker et al., 1997).

In photoreduction experiments, it has been shown that the fastest rate of Fe(III) reduction is achieved in the presence of certain DOM components such as glucaric acid (GA), which can act as an electron donor (Kuma et al., 1992, 1995). A similar type sugar acid, 0.8 μM gluconic acid, was

detected in surface water during a spring bloom in Funka Bay (Japan) (Kuma et al., 1992, and references therein). GA can form strong complexes with Fe(III) in seawater (Log $K_{FeL} = 24$; Kuma et al., 1995).

In a system containing GA, a simplified photoreduction scheme might be

$$\text{Fe(III)}-\text{GA complex} + h\nu \Rightarrow \text{Fe(II)} + \text{GA}* \quad (1)$$

(ligand to metal charge transfer (LMCT)). GA* is oxidation product of GA.

$$\text{Fe(II)} + \text{GA}* \Rightarrow \text{soluble Fe(III)}-\text{GA} \quad (2)$$

(Kuma et al., 1995).

DOM is both a potentially important electron source for photoreductive Fe(II) production and an important source for secondary reducing radicals such as $O_2^{\bullet -}$ (Faust and Zepp, 1993), while at the same time being important for the re-oxidation of Fe(II) to Fe(III). This duality results from DOM being a source of many photo-produced radicals (e.g. H_2O_2, $HO_2^{\bullet\prime}$, $O_2^{\bullet -}$ and $OH^{\bullet}$) that can oxidize Fe(II).

The roles of DOM and light on the speciation, photochemistry and complexation of iron necessarily has a profound impact on iron availability for phytoplankton. We therefore designed a deck experiment on HNLC water from the Southern Ocean. In these experiments we tested the effect of iron enrichment and photoreduction on the phytoplankton growth rate in the presence of GA under natural light with different wavelength ranges: PAR (400–700 nm), and UVAB and PAR (280–700 nm). In this paper we have focused on the results of experiments from WIE water. The results of experiments from SIE have not been presented here, but mentioned only briefly for the purpose of giving a more holistic picture.

2. Materials and methods

The incubation experiments were performed on S.A. *Agulhas* during a cruise in December 1997 and January 1998. The study area was in the locations of the winter ice edge (WIE) and the spring ice edge (SIE) (see Fig. 1 in Turner et al., 2004). The position and depths for water samples to be incubated were determined based on in vivo Chl-*a* and light transmittance measurements. Seawater samples at the WIE (at station D233; 56°30′S, 6°E) were collected from 15 m depth using a peristaltic pump with acid-washed tubes attached to a Kevlar hydrowire. Seawater samples, at station D013 (60°54′S, 05°54′E) in the SIE, were collected from 30 m depth (Chl-*a* maximum) using an acid-washed 30 l Go-Flo sampler deployed on Kevlar hydrowire.

The incubation carboys had been sequentially washed, first with microdetergents, then with Milli-Q water, methanol, Milli-Q water and 3 M HCl and kept for 2 weeks in 0.1 M Ultrapure HCl. Finally, all carboys were rinsed with copious amounts of Milli-Q water.

Incubations were performed in 12 l polycarbonate (PC) carboys (for PAR) and polyethylene (PE) bags (for UVAB–PAR). PE bags and PC carboys transmitted wavelengths >220 nm and >370 nm, respectively. The enrichments were iron (Fe), iron + glucaric acid (FeGA), and no addition (control, C) replicates (two carboys or bags for each treatment) for PAR and UVAB–PAR irradiance, respectively. Additional incubations under UVA–PAR were performed in addition to PAR and UVAB–PAR in SIE. In these incubations, UVB was excluded by using a Mylar filter (which transmits wavelength >320 nm). The GA solution was cleansed of iron by passing it through a Chelex-100 column, which was previously prepared and washed with 1 l of Milli-Q water to minimize the possible leakage of functional groups of Chelex-100 into GA solution. In order to outcompete other natural organic complexes in seawater, at least at the beginning of the experiments, the FeGA mixture was prepared 2 days before addition. First additions of Fe, and FeGA to the incubation carboys were done after 24 h of phytoplankton acclimatization to deck conditions. Iron was added as $FeCl_3$ solution (pH 2) to make a final concentration of $\geqslant 5$ nM. Iron–GA mixture was added to a final concentration of $\geqslant 5$ nM Fe and to make a final GA concentration of 1.2 μM. For every light treatment, there were Fe, FeGA and control treatments. Additions of Fe and FeGA to WIE water were done at the beginning

of the experiment and on day 10 (+3 nM Fe and 1.2 μM GA) of the 14-day-long experiment. The amount of added Fe was determined according to natural iron fluxes to the oceans. The atmospheric fluxes to the Atlantic Ocean range from 18 mmol $m^{-2} y^{-1}$ west of North Africa to 0.02 mmol $m^{-2} y^{-1}$ in the Atlantic sector of the Southern Ocean (Duce and Tindale, 1991). Similarly, fluxes of iron to the Pacific Ocean also ranged from ca. 18 mmol $m^{-2} y^{-1}$ east of Japan to 0.02 mmol $m^{-2} y^{-1}$ in the equatorial Pacific. For 50 m mixing-layer depth, the maximum natural atmospheric input of Fe to the ocean would be ca. 1 nmol $l^{-1} d^{-1}$. Additions of 5+3 nM iron for 14-day incubations (ca. 0.5–0.6 nmol $l^{-1} d^{-1}$) lie between the range of atmospheric iron inputs found in the Pacific and Antarctic Oceans. Moreover, the added iron may have been removed by precipitation or by adsorption onto the wall of carboys and become less available to phytoplankton. Additionally, photochemically produced Fe(II) may have been re-oxidized quickly. Therefore, we added extra iron and GA to meet the increased demand of iron when phytoplankton began growing. The amount of added GA (1.2 μmol l^{-1}) was chosen higher than the detected value of similar hydroxycarboxylic acid in nature (ca. 0.8 μmol l^{-1}; Nakabayashi et al., 1993, cited in Kuma et al., 1995) in order to ensure the presence of GA during incubations. The carboys were incubated on the helicopter deck. All incubation carboys and PE bags were covered by PE bags and carefully sealed to prevent contamination. PVC grey mosquito nets were used for irradiance adjustment. Incubation light was kept around 50% of ambient PAR. Running seawater was used to keep the incubation temperature close to the ambient level (1 °C). On occasions it rose to 1–2 °C higher than ambient temperature.

PC carboys and PE bags had tap systems that were tightly closed during incubation. All samples were drawn either by an all-polypropylene (PP) syringe connected to a Teflon tube or by a peristaltic pump without opening the carboys, through the sample out port. The air input taps were connected with a double 0.2 μm Teflon filter to keep out contamination in the air during sampling and kept closed during incubations. All tubing was previously acid-washed Teflon or Bevaline. Sampling during the experiment with WIE water was done in a dust-free (class 100) container through tapping tubes, without opening the carboys and bags. Fe(II) was determined with a stopped-flow luminol chemiluminescence meter (SFL-CL) (O'Sullivan et al., 1995; King et al., 1995; Powell et al., 1995) immediately after sampling and filtration through a 0.4 μm filter in an all-PP syringe filter holder in a clean container. This method has a detection limit of 0.06 nM Fe. Measurements of in vivo fluorescence were done immediately by using a Turner Design fluorometer. Ten replicates were done repeatedly for each sample. Samples for POC and PON and Chl-*a* were filtered on pre-combusted GF/F filters, packed in pre-combusted aluminum foil, and stored at −18 °C until analysis in the shore laboratory. POC and PON were determined on a CHN Analyzer (Carlo Erba). For Chl-*a* determinations, samples filtered onto GF/F filters were extracted with 90% methanol for 12 h and analyzed by a Turner Design fluorometer. Total peroxides (H_2O_2 and organic peroxides) concentrations were measured with a spectrofluorometer (excitation: 313 nm; emission: 400 nm) using horseradish peroxidase and dimerization of *p*-hydroxyphenylacetic acid (Miller and Kester, 1994b, and references therein). Organic peroxides were measured similarly with the addition of enzyme catalase together with horseradish peroxidase.

Nano- and picophytoplankton were counted by flow cytometry. The microphytoplankton were counted by light optical microscope. Phytoplankton samples from the incubation carboys were fixed by Lugol and formaline solutions (20%) in 500 and 150 ml bottles. After arrival at Trondheim Biological Station, samples were transferred to the sedimentation chambers. Volumes of 2, 10, 30 and 50 ml were selected depending on phytoplankton abundance. The samples were kept in sedimentation chambers for at least 3 days. Counting and species determination were done by inverse microscopy. At least 24 repeated counts were done for each sedimentation chamber.

Samples for bacterial abundance were preserved in formaldehyde (2% final concentration) and

were analyzed by flow cytometry as described by del Giorgio et al. (1996). All analyses were performed on board within 1 week of sampling. Bacterial production was measured according to the Leucine incorporation method (Smith and Azam, 1992).

3. Results and discussion

The total background Fe concentration at a depth of 15 m in WIE was 0.47 ± 0.13 nM ($n = 3$). Daily maximum irradiation of UVA, UVB and PAR was in the range of 21.1–53.8, 1.6–4.2 and 125–415 W m^{-2}, respectively (Wängberg et al., 2004).

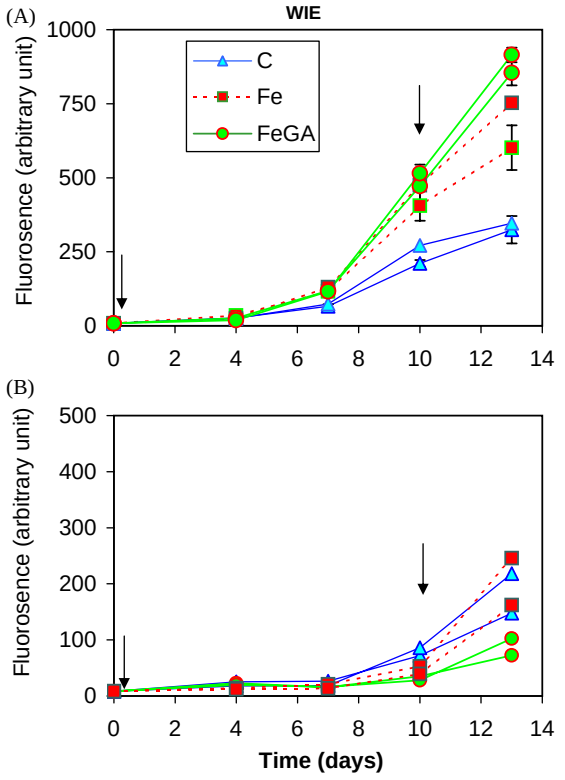

Fig. 1. In vivo fluorescence (IVF) data for phytoplankton growth following incubations in the location of the winter ice edge (WIE) of the Southern Ocean under IVF data for phytoplankton growth following the incubations of WIE seawater under PAR (A) and UVAB–PAR (B). The arrows indicate additions of Fe and FeGA.

3.1. *In vivo fluorescence and phytoplankton response to iron addition*

In vivo fluorescence of different treatments started to diverge on day 7 (Fig. 1A). There was a very clear response from Fe and FeGA treatments compared to the controls. In vivo fluorescence was significantly higher in Fe and FeGA treatments (t-test, $P < 0.05$). FeGA treatments yielded the highest in vivo fluorescence at the end of the experiments (t-test, $P < 0.05$). In UVAB–PAR treatments, the highest in vivo fluorescence was observed up to day 10 in the control (Fig. 1B) and the lowest in vivo fluorescence in the FeGA treatments. Differences of in vivo fluorescence between control and FeGA treatments after day 10 were siginificant ($P < 0.05$). At the end of the 14-day-long incubations, in Fe and FeGA treatments under PAR, the dominating phytoplankton species were *Pseudonitzschia* spp., *Nitzschia* spp. and *Phaeocystis* spp. A considerable increase in the number of *Rhizosolenia* spp. was observed in FeGA–PAR treatment. In the control treatments, the predominant species was *Phaeocystis* spp. A shift from nano–picophytoplankton to microphytoplankton was evident in Fe and FeGA treatments under PAR (Fig. 2A and B). Under UVAB–PAR, *Phaeocystis* spp. was dominant. After the enrichment with Fe and FeGA, the number of nano–picophytoplankton also increased considerably (Fig. 2B).

These data suggest that Fe and FeGA additions dramatically alter the species composition from nano–pico to diatoms >20 μm in the WIE (Fig. 2). This was particularly pronounced in FeGA treatments. The increase in diatoms after the addition of Fe is in agreement with previous Fe enrichment studies in HNLC regions (Coale, 1991; van Leeuwe et al., 1997; Scharek et al., 1997).

Our results suggest that microphytoplankton (mainly diatoms >20 μm) respond favorably to the addition of FeGA and Fe in the WIE waters. Presumably, nano–pico plankton has an advantage under Fe-limited conditions, due partially to their relatively low iron requirements (Sunda et al., 1991) and/or their greater surface area : cell volume ratio, ensuring more efficient Fe uptake. Under UVAB–PAR, however, FeGA treatments

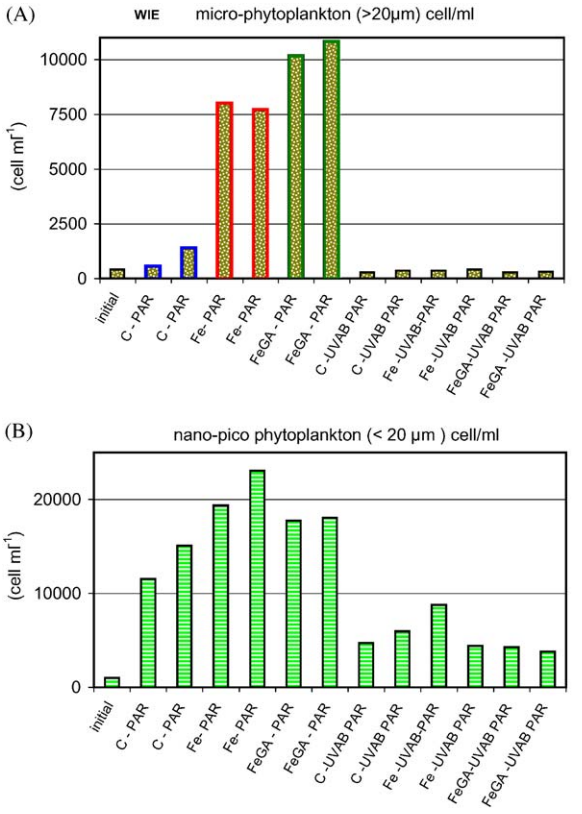

Fig. 2. Initial and final cell densities (cell ml^{-1}) for micro-phytoplankton (A) and nano–picophytoplankton (B) for each treatment and controls for incubation in WIE.

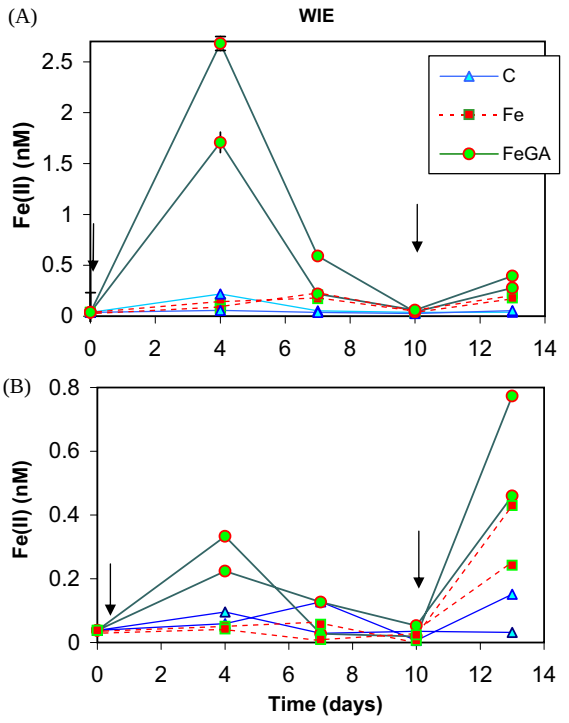

Fig. 3. Photoproduction of Fe(II) in the incubations of WIE seawater under PAR (A) and UVAB–PAR (B). Vertical arrows indicate additions of Fe and FeGA.

yielded the lowest phytoplankton biomass. This has also been observed in the SIE (data not shown). Under UVAB–PAR, FeGA may enhance the harmful effects of UV, probably due to photochemical reactions in which FeGA plays a role. It has also been reported that nutrient stress may cause increased release of organic matter (Lancelot and Billen, 1985; Verity et al., 1988), that is, after enrichment with FeGA, under UVAB–PAR, phytoplankton may release less UV-protective organic matter, thus less protection against UV.

3.2. *Fe(II), organic peroxides and H_2O_2*

After the addition of FeGA, Fe(II) increased dramatically (Fig. 3A), especially under PAR. On day 4, concentrations of Fe(II) were 1.7 and 2.6 nM in the FeGA treatments under PAR. The high level of Fe(II) on day 4 indicates photoreductive Fe(II) production due to the presence of GA. When the phytoplankton began growing, the Fe(II) concentration started to decrease, reaching the detection limit on day 10. Then, new additions ($+3$ nM Fe, $+3$ nM-1.2 µM FeGA) were made to meet the increased Fe demand. Fe(II) was still detectable 3 days after the second addition (Fig. 3A and B). Fe(II) concentrations in the FeGA treatment under UVAB–PAR varied similar to those of PAR treatments, albeit Fe(II) concentrations under UVAB—PAR–FeGA treatments were much lower than under PAR–FeGA treatments (Fig. 3B).

Peroxide concentration (H_2O_2 + organic peroxides) under PAR was low at the beginning and then increased to 150–250 µmol m^{-3} on day 10, and decreased to 15–40 µmol m^{-3} on day 13 (Fig. 4A and C) in all treatments. In the controls, organic peroxides were a little higher than in iron

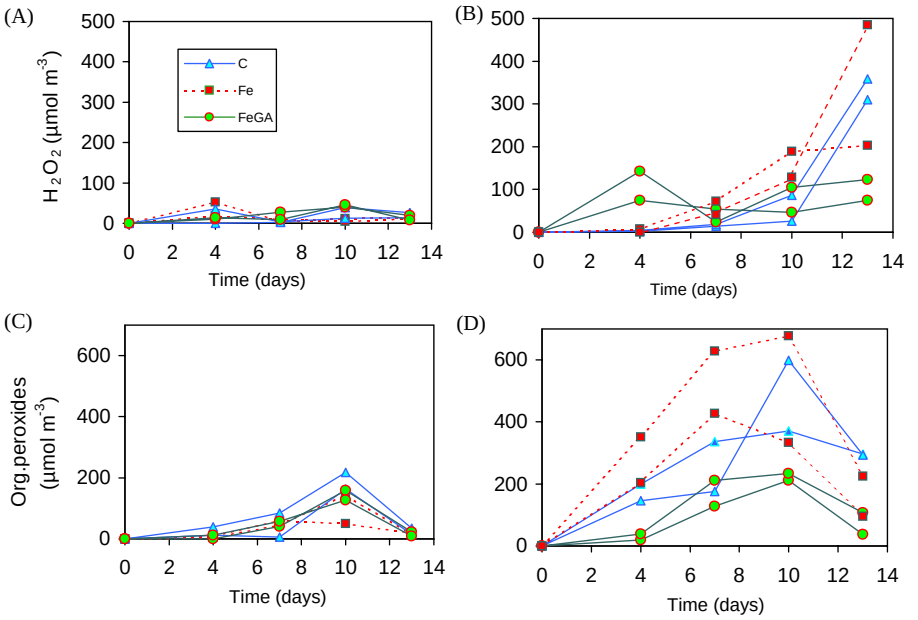

Fig. 4. Concentration of H_2O_2 under PAR (A) and UVAB–PAR (B), and organic peroxides under PAR (C) and UVAB (D) in the incubations of WIE seawater.

treatments. Under UVAB–PAR, the highest concentrations of H_2O_2 and organic peroxides were observed in the Fe treatments (Fig. 4B and D). The lowest concentrations of H_2O_2 and organic peroxides were observed in FeGA treatments. The organic peroxides concentration increased when there was little phytoplankton activity and started to decrease at the end of incubations in all treatments under UVAB–PAR. Concentrations of H_2O_2 and organic peroxides in all treatments of SIE were almost one order of magnitude lower than in the treatments of WIE.

After the formation of Fe(II), components of DOM, in addition to GA, might be responsible for keeping Fe(II) in solution. Some DOM compounds which are produced from phytoplankton could be important for Fe(III) photoreduction and some others could cause retardation of oxidation of Fe(II) and keep Fe(II) in solution by complexation. In order to understand the extent of primary photochemical reduction of Fe by the help of GA it is necessary to estimate the rate of oxidation/reduction reactions. We adopted first-order reversible photochemical oxidation/reduction reaction equations suggested by Kuma et al. (1995):

$$\text{Fe(III)GA (dissolved)} + h\nu \;\leftarrow k_{ox}\; k_{red} \rightarrow \text{Fe (II)} + \text{GA}*. \quad (3)$$

The Fe(II) concentration as a function of time can be written as

$$[\text{Fe(II)}]_t = \{\{k_{red}[\text{Fe(III)GA}]_0\}/(k_{red}+k_{ox})\}[1-\exp\{-(k_{red}+k_{ox})\,t\}], \quad (4)$$

where $[\text{Fe(III)GA}]_0$, $[\text{Fe(II)}]_t$, k_{red} (min^{-1}) and k_{ox} (min^{-1}) are the concentrations of Fe(III)GA at $t=0$ and Fe(II) at time t, and the rate constants of the forward (reduction) and reverse (oxidation) reactions, respectively. Kuma et al. (1995) reported values of k_{ox} and k_{red} at different temperatures (5, 10 and 15 °C) and different irradiances (1400, 1900 and 2300 µmol m^{-2} s^{-1}). k_{red} is independent of temperature and increases linearly with increasing irradiance (I_L). We obtained k_{red} dependence on irradiance ($k_{red}=0.00004I_L-0.022$; $R^2=0.996$) and k_{ox} dependence to temperature ($k_{ox}=0.0087T+0.03$; $R^2=0.99$) from the data of Kuma et al. (1995). These estimations depend

on the assumptions that k_{red} and k_{ox} are linearly related to irradiance (I_L) and temperature (T), respectively, in extrapolated zones. From these approximations we calculated that maximum steady-state concentration of Fe(II) could reach 40–50% of added FeGA concentrations at 0 and $-1\,^{\circ}C$ under 50% of ambient irradiance.

In the WIE, steady-state Fe(II) concentrations were ca. 32–50% and 5% of the added Fe(III) in PAR–FeGA and in UVAB–FeGA treatments, respectively. These results imply that Fe photoreduction under PAR seems to be more efficient than the secondary oxidation of Fe(II) by photochemically produced radicals. The difference in Fe(II) at the beginning of incubations between PAR and UV treatments was probably related to re-oxidation of photoreduced Fe(II) by photochemically produced radicals under UV treatments. Relatively high levels of H_2O_2 and organic peroxides in UV treatments both in WIE and SIE (data not shown) support this.

At high pH (typical for strong photosynthesis), the rate of secondary reduction of Fe(III) by the photochemically produced radical ($HO_2^{\bullet}/O_2^{\bullet-}$) increases (Voelker et al., 1997). This rate is at least 15 times higher than that of the Fe(II) re-oxidation reaction with $HO_2^{\bullet}/O_2^{\bullet-}$ (King et al., 1995), implying that, at natural conditions under PAR, Fe(III)GA could be a considerable source of Fe(II) and a sink for $HO_2^{\bullet}/O_2^{\bullet-}$. The presence of Fe does not seem to have been significant for the formation of H_2O_2 and $HO_2^{\bullet}/O_2^{\bullet-}$.

Our results under PAR neither suggest that organic peroxide formation depends on the presence of Fe, nor that there is a relationship between phytoplankton activities and organic peroxides in WIE or SIE. However, in the WIE experiments under UVAB–PAR, the H_2O_2 concentration generally shows increase with phytoplankton productivity. In the SIE experiments, despite the fact that the concentrations of H_2O_2 and organic peroxides in all treatments of SIE were almost one order of magnitude lower than in WIE, the trends of H_2O_2 and organic peroxides variations, especially under UVAB–PAR treatments, are almost the same as in WIE. The lowest levels of H_2O_2 and organic peroxides were observed in FeGA as the lowest values of POC and Chl-*a*. Organic peroxides levels increased when there was no phytoplankton activity and decreased with increasing phytoplankton growth at the end of incubations in all treatments under UVAB–PAR. Thus, FeGA may have inhibited the formation of organic peroxides, or some organic peroxides may have been used to oxidize Fe(II) back to Fe(III) by photochemically produced radicals originating from organic peroxides. This interpretation is supported by the relatively low concentration of Fe(II) in FeGA treatments under UVAB–PAR compared to under PAR. In the FeGA treatments under UVAB–PAR, the same process probably acted as a sink for photochemically produced peroxides and Fe(II). The most probable reaction is

$$\mathrm{Fe\ (II)} + \mathrm{H_2O_2} \Rightarrow \mathrm{Fe\ (III)} + \mathrm{OH^-} + \mathrm{OH^{\bullet -}}. \quad (5)$$

It seems that, in FeGA treatments, the oxidation of Fe(II) with H_2O_2 (Fenton reaction) may have been an important source of $OH^{\bullet}$ under UVAB–PAR. Hence, it may have caused oxidation of UV-protective DOM. This is also supported by the relatively low concentrations of H_2O_2 and organic peroxides, and the low phytoplankton productivity and biomass in the FeGA treatment compared to Fe and the control treatments.

The secondary reducing mechanisms, such as fast reduction of dissolved Fe(III) by the superoxide radical (Voelker and Sedlak, 1995), may also contribute to a build-up of the high steady-state Fe(II).

On the other hand, some DOM fractions may inhibit the re-oxidation of Fe(II) by oxidative radicals in two possible ways: (a) Organic matters are themselves oxidized by photochemically produced radicals, that is, Fe(II) oxidation by photochemically produced radicals is out-competed by oxidation of DOM by photochemically produced radicals. (b) Fe(II) is stabilized by organic complexation against oxidation by photochemically produced radicals.

3.3. Carbon and nitrogen assimilation: POC and PON

Under PAR, particulate organic carbon (POC) in all treatments began to diverge on day 7 until

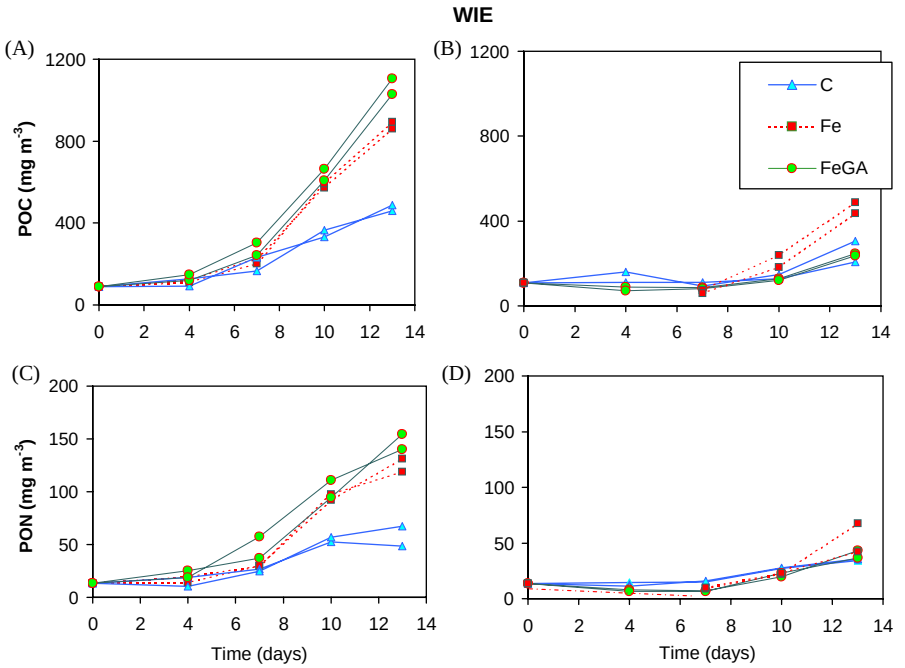

Fig. 5. Concentrations of POC under PAR (A) and UVAB–PAR (B), and PON under PAR (C) and UVAB–PAR (D) over time in iron-enrichment experiments in water from WIE.

the end of the experiments (Fig. 5A) and POC levels were significantly higher in Fe and FeGA treatments (*t*-test, $P<0.05$) compared to controls. POC values on day 13 in FeGA and Fe treatments were about. 2.2 and 1.9 times higher, respectively, than the POC in the controls ($P<0.05$). Moreover, on day 13, POC levels were significantly higher in FeGA ($P<0.05$) compared to POC levels in Fe treatments (Fig. 5A). Under UVAB–PAR, carbon build-up was very low in all treatments. However, POC in Fe treatments was ca. 1.8 times higher than that in both FeGA and control treatments ($P<0.05$). The lowest POC was detected in FeGA treatment under UVAB–PAR (Fig. 5B).

Particulate organic nitrogen (PON) showed similar trends as POC. The final PON levels were significantly higher in Fe and FeGA treatments ($P<0.05$). Under PAR, the difference of PON ($90\,mg\,m^{-3}$) between FeGA and controls on day 13 was higher than that between Fe and control treatments ($67\,mg\,m^{-3}$) (Fig. 5C). PON values on day 13 in FeGA and Fe treatments were ca. 2.6 and 2.2 times higher than that in the control, respectively. Under UVAB–PAR, the build-up of *N* was also very low in all treatments (Fig. 5D)

Primary production rates (based on increases in POC) in Fe and FeGA treatments under PAR were similar and ca. 2.5 times higher than that in the control on day 10. (Fig. 6). On day 13, the primary production rates in the Fe treatments were again ca. 2.5 times higher than that in the control. On the other hand, production rates in the FeGA were ca. 3.5 times higher than the controls. In the SIE, under UVAB–PAR, FeGA and control treatments also yielded the lowest and highest POC buildup, respectively, as in FeGA and C treatments in WIE under UVAB–PAR.

3.4. Chlorophyll-a

Under PAR, Chl-*a* enhancement clearly resulted from the additions of Fe and especially FeGA in our experiments (Fig. 7A). The levels of Chl-*a* on days 10 and 13 were significantly higher than the levels of Chl-*a* in the controls ($P<0.05$). Fe and FeGA treatments showed the largest Chl-*a*

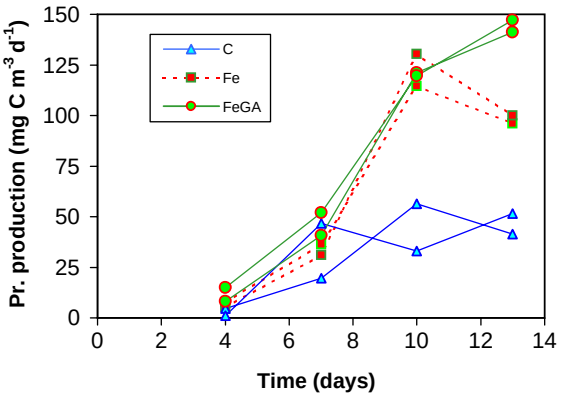

Fig. 6. Estimation of primary production as a function of time based on POC data for all phytoplankton communities in WIE incubations for all PAR treatments.

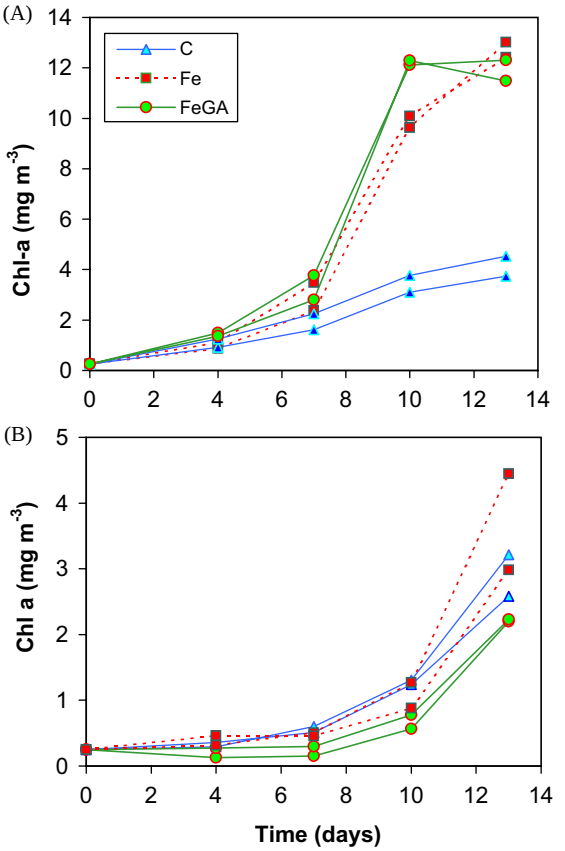

Fig. 7. Chl-*a* increase under PAR (A) and UVAB–PAR (B) in water from WIE.

increase between days 7 and 10. After day 10, the increase was tempered in the Fe treatments and stopped in the FeGA treatments. Chl-*a* concentrations in day 10 in the FeGA and Fe treatments were ca. 3.6 and 2.9 times higher than in the controls, respectively. The highest Chl-*a* production rate ($3.16\,\mathrm{mg\,Chl\text{-}a\,m^{-3}\,d^{-1}}$) was observed between days 7 and 10 in the FeGA treatments, and was ca. 2.3 and $0.5\,\mathrm{mg\,Chl\text{-}a\,m^{-3}\,d^{-1}}$ in the Fe and control treatments, respectively. That is, Chl-*a* production rates in the FeGA and Fe treatments between days 7 and 10 were ca. 6 and 4.6 times higher than that in the control, respectively.

Chl-*a* synthesis was apparently enhanced by Fe enrichment (Fe and FeGA) (Fig. 8A). However, Chl-*a* values under UVAB–PAR are quite low relative to values for corresponding treatments under PAR. In contrast to under PAR treatments, the Chl-*a* concentration began to increase after day 10. FeGA treatments under UVAB–PAR yielded the lowest Chl-*a* build up (Fig. 7B).

Chl-*a* increases resulting from the addition of Fe and FeGA were also evident in SIE PAR and UVA–PAR incubations (data not shown). The enhanced Fe(II) concentration apparently also had an impact on phytoplankton growth in SIE although it does not change the species composition. In SIE incubations, under UVAB–PAR, the highest Chl-*a* build-up was observed in control treatments, and the lowest Chl-*a* build-up was in FeGA treatment as it was in FeGA treatments in WIE incubations under UVAB–PAR.

The ratio of Chl-*a* production rates (PR-Chl-*a*) between FeGA and the control, and between Fe and the control treatments (FeGA/control and Fe/control) during exponential growth in WIE under PAR were higher than the corresponding ratios for carbon production rates (PR-POC):

$$\{\mathrm{PR-Chl-}a_{\mathrm{FeGA}} : \mathrm{PR-Chl-}a_{\mathrm{cont.}}\} : \{\mathrm{PR-POC_{FeGA}} : \mathrm{PR-POC_{cont.}}\} \cong 2.4$$

$$\text{and } \{\mathrm{PR-Chl-}a_{\mathrm{Fe}} : \mathrm{PR-Chl-}a_{\mathrm{cont.}}\} : \{\mathrm{PR-POC_{Fe}} : \mathrm{PR-POC_{cont.}}\} \cong 1.8.$$

This possibly indicates that Fe enrichment first triggered Chl-*a* synthesis and then the biomass

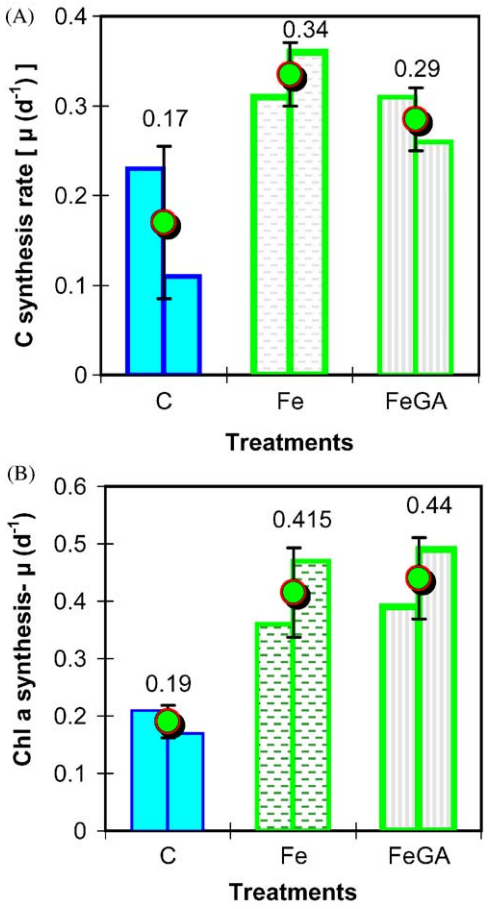

Fig. 8. Rates of Chl-*a* (A) and carbon synthesis during exponential growth in water from WIE under PAR.

increase. This effect was most pronounced in the FeGA treatments in WIE under PAR. Moreover, the rates of Chl-*a* synthesis in FeGA were slightly higher than those in the Fe treatments (Fig. 8A). The C:Chl-*a* ratios indicate that production of Chl-*a* is fastest in the Fe treatments, especially in the FeGA treatments in WIE under PAR.

3.5. Nutrients

Our results showed a significant increase of nutrient uptake by phytoplankton in Fe and FeGA treatments compared to the controls under PAR (Fig. 9A and B) (*t*-test, $P<0.05$ for both NO_3+NO_2 and Si). Towards the end of the experiment (day 13), removal of NO_3+NO_2 in FeGA, Fe, and control treatments were ca. 24, 23 and 12 mmol m^{-3}, respectively. Similarly, Si in FeGA, Fe and controls treatments decreased from ca. 60 mmol m^{-3} to ca. 15, 21 and 33 mmol m^{-3}, respectively (Fig. 9B). The removal of Si in FeGA was significantly higher than the removal of Si in Fe treatments ($P<0.05$). Despite the fact that diatoms species were not dominant in the controls under PAR, removal of Si was considerably high in control treatments (Fig. 9B). During the incubations under PAR, Si removal values against C build-up (ΔSi:ΔPOC) are 0.9 ± 0.03, 0.6 ± 0.02 and 0.57 ± 0.01 for control, Fe and FeGA treatments, respectively. The highest ΔSi:ΔPOC ratio in control indicates that Si uptake is increased with Fe stress. This is in agreement with the observation that diatoms from low-Fe waters do have high Si cell quotas (Hutchins and Bruland, 1998; Boyle, 1998). The decrease of NO_3+NO_2 was between ca. 5 (in FeGA) and 8 mmol m^{-3} (in Fe and control) under UVAB–PAR (Fig. 9C). These were quite low values compared to the decrease in NO_3+NO_2 in all treatments under PAR. Removals of Si under UVAB–PAR are ca. 10, 8 and 7 mmol m^{-3} in the control, Fe and FeGA treatments. These are low, nevertheless considerable values. Although the diatom community was not high in these treatments UV stress might have caused heavier silicification per diatom as light, temperature, N and iron stress (Flynn and Martin-Jézéquel, 2000) in the treatments under UVAB–PAR.

3.6. Bacteria

Under PAR, both the FeGA and the Fe treatments resulted in an enhanced yield of bacterial cells. The average cell counts were approximately 2.4-and 2-fold of the control levels, respectively (Fig. 10A). At the end of experiment, bacterial production in Fe and FeGA treatments was significantly higher than that of controls ($P<0.05$). There was a strong increase in bacterial productivity in Fe treatments compared to the production in the FeGA treatment and in the controls (Fig. 10c). This increase in bacterial production coincided with a decrease in primary

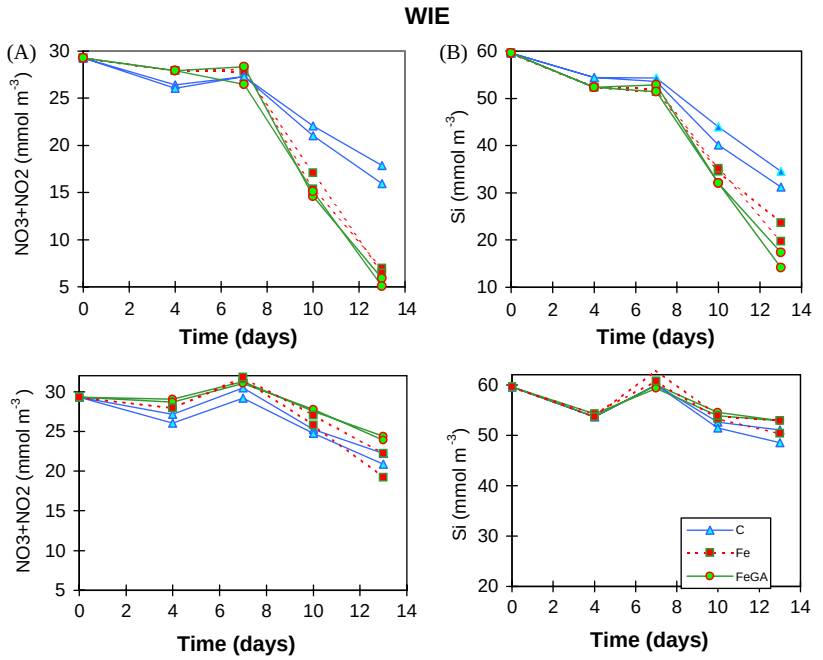

Fig. 9. The decrease in concentrations of $NO_3 + NO_2$ (A) and Si (B) under PAR, and $NO_3 + NO_2$ (C) and Si (D) under UVAB–PAR over time in water from WIE.

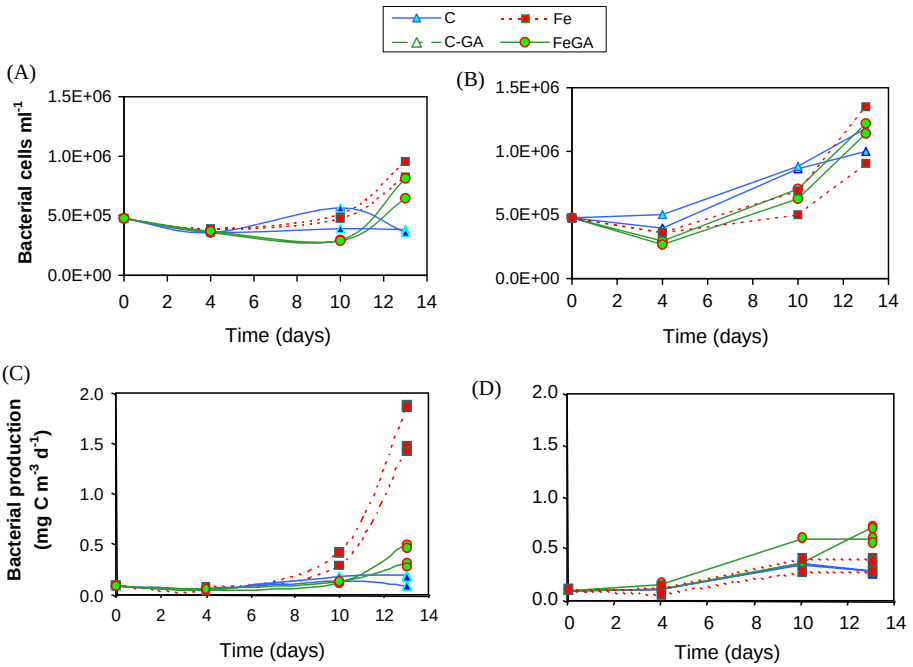

Fig. 10. Bacterial cell numbers under PAR (A) and UVAB–PAR (B) in water from WIE, and bacterial production under PAR (C) and UVAB–PAR (D) in water from WIE.

productivity in incubations enriched with Fe under PAR (Fig. 6).

Under UVAB–PAR, bacterial density (Fig. 10B) did not differ between treatments. On the other hand, at the end of experiment, bacterial productivity in FeGA (Fig. 10D) was significantly higher ($P<0.05$) than that in the Fe treatments and controls. A moderate increase both in bacterial cell density and bacterial productivity was observed in the last part of the incubation period for all treatments.

The role of bacteria in the elemental cycles, the regeneration of nutrients, and in the trophodynamics of marine ecosystems is widely recognized (Pakulski et al., 1996; Tortell et al., 1999). However, in most of the deck experiments related to iron-deficient HNLC zones, data on bacterial responses to addition of Fe have been obtained in very few studies (Pakulski et al., 1996; Tortell et al., 1999). The stimulatory effects of iron enrichment on bacterial growth could be both direct and indirect results of the Fe enrichment; Fe could directly increase the bacterial growth by being an essential nutrient, while it also increases the amount of bioavailable organic matter as a result of Fe-induced phytoplankton growth and organic matter release.

In Fe treatments under PAR in the WIE, there was much stronger bacterial response to the iron enrichment compared to the FeGA treatments, even though the FeGA treatments were enriched with extra organic matter (glucaric acid). However, the considerably higher phytoplankton growth in this treatment (compared to the Fe treatment) suggests that bacteria and phytoplankton may compete for iron, and that the speciation of iron influences the ability of these organisms to compete for this nutrient. There are some reports showing an increase in bacterial growth rate with iron experiments conducted in the dark (no extra organic matter from enhanced photosynthetic production) (Pakulski et al., 1996). Hence, it is likely that the direct effect of iron (especially Fe (III) in Fe treatments) on bacterial production is important. Our data are not sufficient to make conclusive suggestions on the role of Fe on bacterial growth and the role of bacteria in the cycling of Fe in the euphotic layer of the Southern Ocean. However, we believe that the role of bacteria in the biogeochemical cycling of Fe deserves further attention, particularly with respect to possible competition between bacteria and phytoplankton for iron as a scarce resource.

3.7. Total dissolved inorganic carbon (ΣCO_2)

ΣCO_2 was determined only for the WIE experiments. The significant decrease in ΣCO_2 was observed in FeGA treatments (ca. 140 mmol m^{-3} during incubation) and in Fe (ca. 100 mmol m^{-3}) treatments under PAR (Fig. 11). ΣCO_2 decrease in control treatments was around 40 mmol m^{-3}. Under UVAB–PAR, a small decrease in ΣCO_2, ca. 13 mmol m^{-3} ,was observed in the controls. Fe additions did not cause any change in ΣCO_2.

When we compare POC accumulation and decrease in ΣCO_2 in all treatments in WIE experiments, the ratio of POC accumulation to ΣCO_2 decrease in FeGA, Fe and control under PAR is found to be 0.59, 0.64 and 0.73, respectively. The difference between ΣCO_2 decrease and accumulated POC can be attributed to the production of dissolved organic carbon (DOC), implying that DOC production in FeGA, Fe and control under PAR in WIE experiments may constitute 41%, 36% and 27% of total fixed carbon, respectively. This is important to understand the effect of Fe enrichments on CO_2 flux in euphotic zones. Since biologically labile DOC will eventually turn back relatively quickly into the pool

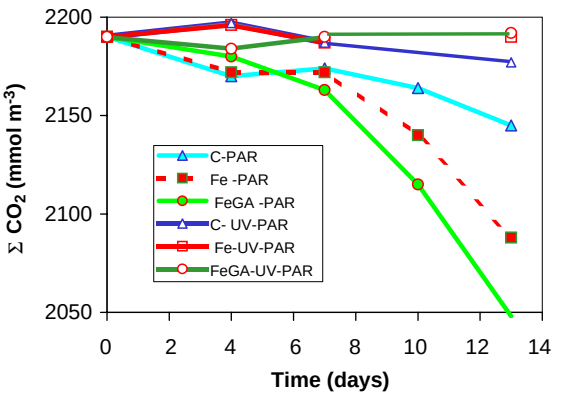

Fig. 11. Decreases in total dissolved inorganic carbon (ΣCO_2) under PAR and UVAB–PAR in iron-enrichment experiments in water from WIE.

of ΣCO_2, and only refractory DOC and sinkable POC contributes to the export of ΣCO_2 from surface water to deep water and sediment as a POC, it is important to understand the qualitative and quantitative DOC production compared to POC production due to enhancement of phytoplankton productivity with the enrichment of Fe.

4. Conclusions

Our enrichment experiments indicate that Fe and FeGA enrichments significantly increase phytoplankton biomass build-up and cause a higher growth rate compared to control treatments in the WIE under PAR (and, to some extent, in SIE under UVA–PAR). This implies that iron has an important role as a limiting factor, especially in the WIE of the Southern Ocean. Most of the biomass increase in Fe and FeGA treatments was due to diatoms $>20\,\mu m$, suggesting that this diatom community was particularly limited by the supply of Fe.

In the WIE under PAR, Fe stimulated Chl-*a* synthesis prior to carbon build-up. The effect of GA on the availability of Fe appears to be considerable. This could be explained by the effects of GA on the Fe(III) photoreduction by primary photochemical processes. Secondary processes (by photochemically produced radicals) may play some role for observable Fe(II) but their mechanisms are not yet fully understood. These mechanisms may enhance the production of available iron and make Fe(II) available from a pool of Fe(III) which is already present.

Apparently, the primary and secondary photochemical reduction of Fe(III) and re-oxidation of Fe(II) by photochemically produced radicals are affected by the spectral quality of light, speciation of Fe(III) and DOM, as well as by competitive reactions of DOM, Fe(III) and Fe(II) with photochemically produced radicals.

The role of iron for the formation of peroxide and hydroxide–superoxide radicals seems insignificant under PAR. On the contrary, under UV secondary oxidation of Fe(II) by photochemically produced radicals probably is an important sink for both Fe(II) and H_2O_2.

Related to UV and PAR dependence of iron photoreduction, our preliminary data did not show whether any particular wavelength band can reduce Fe(III) more effectively than others. Contrary to expectations of more effective photoreduction of Fe(III) in both UVB and UVA (based on data from inorganic Fe photoreduction experiments; Stumm and Morgan, 1996), our results show that the presence of GA causes efficient photoreduction of Fe(III) under PAR as well as in UV.

Both in the WIE and SIE, in incubations exposed to UVAB–PAR, FeGA treatments invariably yielded the lowest phytoplankton productivity. Thus the protective mechanism of phytoplankton to UV seems to be affected by FeGA. Fe photoreduction may enhance the negative effects of UV, contrary to the anticipation that the detrimental effects of UVB in the Southern Ocean could be counteracted by the photoreduction of iron (Palenik et al., 1991) as a result of increased photoreductive dissolution of Fe(III) under UV. This point needs further investigation.

Acknowledgments

We thank and acknowledge Sten-Åke Wängberg for providing us with his light data. We thank chief scientist David Turner and the rest of the scientific party, especially Wilhelm Granéli and Fred Sörensson for their help. We are indebted to Melissa Chierici for her involvement in the total inorganic carbon determination. We thank Eiliv Steinnes for critically reviewing the manuscript and Can Bizsel for his help for the statistical work. We are grateful to the crew of S.A. *Agulhas* for the pleasant cooperation during the cruise. The funding for this work was provided by grants from the Norwegian Polar Institute, Project No. NARE 97/98-3824. Finally, we are grateful to the two anonymous referees for their helpful comments concerning the first version of this paper.

References

Bakker, D.C.E., de Baar, H.J.W., Bathmann, U.V., 1997. Changes of carbon dioxide in surface waters during spring in the Southern Ocean. Deep-Sea Research II 44, 91–127.

Banse, K., 1990. Does iron really limit phytoplankton production in the offshore subarctic Pacific? Limnology and Oceanography 35, 772–775.

Behrenfeld, M.J., Bale, A.J., Kolber, Z.S., Aiken, J., Falkowski, P.G., 1996. Confirmation of iron limitation of phytoplankton photosynthesis in the equatorial Pacific Ocean. Nature 383, 508–511.

Boyle, E., 1998. Pumping iron makes thinner diatoms. Nature 393, 733–734.

Coale, K.H., 1991. Effects of iron, manganese, copper, and zinc enrichments on productivity and biomass in the subarctic Pacific. Limnology and Oceanography 36, 1851–1864.

Coale, K.H., Johnson, K.S., Fitzwater, S.E., Gordon, R.M., Tanner, S., Chavez, F.P., Ferioli, L., Sakamoto, C., Rogers, P., Millero, F., Steinberg, P., Nightingale, P., Cooper, D., Cochlan, W.P., Landry, M.R., Constantinou, J., Rollwagen, G., Trasvina, A., Kudela, R., 1996. A massive phytoplankton bloom induced by an ecosystem-scale iron fertilization experiment in the equatorial Pacific Ocean. Nature 383, 495–501.

del Giorgio, P., Bird, D., Prairie, Y.T., Planas, D., 1996. Flow cytometric determination of bacterial abundance in lake plankton with the green nucleic acid stain Syto 13. Limnology and Oceanography 41, 783–789.

Duce, R.A., Tindale, N.W., 1991. Atmospheric transport of iron and its deposition in the ocean. Limnology and Oceanography 36, 1715–1726.

El Sayed, S.Z., 1988. Productivity of the Southern Ocean: a closer look. Comparative Biochemistry and Physiology 90, 489–498.

Faust, B.C., Zepp, R.G., 1993. Photochemistry of aqueous iron(III)-polycarboxylate complexes: roles in the chemistry of atmospheric and surface waters. Environmental Science and Technology 27, 2517–2522.

Flynn, K.J., Martin-Jézéquel, V., 2000. Modelling Si-N-limited growth of diatoms. Journal of Plankton Research 22, 447–472.

Holm-Hansen, O., Mitchell, B.G., Hewes, C.D., Karl, D.M., 1989. Phytoplankton blooms in the vicinity of Palmer Station, Antarctica. Polar Biology 10, 49–57.

Hudson, R.J.M., Covault, D.T., Morel, F.M.M., 1992. Investigations of iron coordination and redox reactions in seawater using iron-59 radiometry and ion-pair solvent extraction of amphiphilic iron complexes. Marine Chemistry 38, 209–235.

Hutchins, D.A., Bruland, K.W., 1998. Iron-limited diatom growth and Si/N uptake ratios in a coastal upwelling regime. Nature 393, 561–564.

King, D.W., Lounsbury, H.A., Millero, F.J., 1995. Rates and mechanism of Fe(II) oxidation at nanomolar total iron concentrations. Environmental Science and Technology 29, 818–824.

Kuma, K., Nakabayashi, S., Suziki, Y., Kudo, I., Matsunaga, K., 1992. Photo-reduction of iron(III) by dissolved organic substances and existence of iron(II) in seawater during spring blooms. Marine Chemistry 37, 15–27.

Kuma, K., Nakabayashi, S., Matsunaga, K., 1995. Photoreduction of Fe(III) by hydroxycarboxilic acids in seawater. Water Research 29, 1559–1569.

Lancelot, C., Billen, G., 1985. Carbon–nitrogen relationships in nutrient methabolism of coastal marine ecosystems. Advances in Aquatic Microbiology 3, 263–321.

Löscher, B.M., de Baar, H.J.W., de Jong, J.T.M., Veth, C., Dehairs, F., 1997. The distribution of Fe in the Antarctic Circumpolar Current. Deep-Sea Research II 44, 143–187.

Martin, J.H., Gordon, R.M., Fitzwater, S.E., 1990. Iron in Antarctic waters. Nature 345, 156–158.

Martin, J.H., Coale, K.H., Johnson, K.S., Fitzwater, S.E., Gordon, R.M., Tanner, S.J., Hunter, C.N., Elrod, V.A., Nowicki, J.L., Coley, T.L., Barber, R.T., Lindley, S., Watson, A.J., Van Scoy, K., Law, C.S., Liddicoat, M.I., Ling, R., Stanton, T., 1994. Testing the iron hypothesis in ecosystems of the equatorial Pacific Ocean. Nature 371, 123–129.

Miller, W.L., Kester, D., 1994a. Photochemical iron reduction and iron bioavailability in seawater. Journal of Marine Research 52, 325–343.

Miller, W.L., Kester, D., 1994b. Peroxide variations in the Sargasso Sea. Marine Chemistry 48, 17–29.

Millero, F.J., Sotolongo, S., Izaguirre, M., 1987. The kinetics of oxidation of Fe(II) in seawater. Geochimica et Cosmochimca Acta 51, 793–801.

Morel, F.M.M., Hudson, R.J.M., Price, N.M., 1991. Limitation of productivity by trace metals in the sea. Limnology and Oceanography 36, 1742–1755.

O'Sullivan, D.W., Hanson, A.K., Kester, D.R., 1995. Stopped flow luminol chemiluminescence determination of Fe(II) and reducible Fe in seawater at subnanomolar levels. Marine Chemistry 49, 65–77.

Pakulski, J.D., Coffin, R.B., Kelley, C.A., Holder, S.L., Downer, R., Aas, P., Lyons, M.M., Jeffrey, W.H., 1996. Iron stimulation of Antarctic bacteria. Nature 383, 133–134.

Palenik, B., Price, N.M., Morel, F.M.M., 1991. Potential effects of UV-B on the chemical environment of marine organism: a review. Environmental Pollution 70, 117–130.

Powell, R.T., King, D.W., Landing, W.M., 1995. Iron distributions in surface waters of the South Atlantic. Marine Chemistry 50, 13–20.

Sakshaug, E., Holm-Hansen, O., 1984. Factors governing pelagic production in Polar Oceans. In: Holm-Hansen, O., Bolis, L., Gilles, R. (Eds.), Marine Phytoplankton and Productivity, Lecture Notes on Coastal and Estuarine Studies, vol. 8. New York, Springer, pp. 1–18.

Sakshaug, E., Slagstad, D., Holm-Hansen, O., 1991. Factors controlling the development of phytoplankton blooms in the Antarctic Ocean–a mathematical model. Marine Chemistry 35, 259–271.

Scharek, R., van Leeuwe, M.A., de Baar, H.J.W., 1997. Responses of Antarctic Ocean phytoplankton to the addition of trace metals. Deep-Sea Research II 44, 209–227.

Smith, D.C., Azam, F., 1992. A simple economical method for measuring bacterial protein synthesis rates in seawater using 3H Leucine. Marine Microbial Food Webs 6, 107–109.

Stumm, W., Morgan, J.J., 1996. Aquatic Chemistry, third ed. Wiley, New York, 1022pp.

Sunda, W.G., Swift, D.G., Huntsman, S.A., 1991. Low iron requirement for growth in oceanic phytoplankton. Nature 351, 55–57.

Tortell, P.D., Maldonado, M.T., Granger, J., Price, N.M., 1999. Marine bacteria and biogeochemical cycling of iron in the oceans. FEMS Microbiology Ecology 29, 1–11.

Turner, D.R., Bertilsson, S., Fransson, A., Pakhomov, E., 2004. The SWEDARP 97/98 marine expedition: overview. Deep-Sea Research II, this issue [doi:10.1016/j.dsr2.2003.08.006].

van Leeuwe, M.A., Scharek, R., de Baar, H.J.W., de Jong, J.T.M., Goeyens, L., 1997. Iron enrichment experiments in the Antarctic Ocean: physiological responses of plankton communities. Deep-Sea Research II 44, 189–207.

Verity, P.E., Villareal, T.A., Smayda, T.J., 1988. Ecological investigations of blooms of colonial *Phaecystis pouchetii*- I-Abundance, biochemical composition, and metabolic rates. Journal of Plankton Research 10, 219–248.

Voelker, B.M., Sedlak, D.L., 1995. Iron reduction by photoproduced superoxide in seawater. Marine Chemistry 50, 93–102.

Voelker, B.M., Morel, F.M.M., Sulzberger, B., 1997. Iron redox cycling in surface waters: effects of humic substances and light. Environmental Science and Technology 31, 1004–1011.

Wängberg, S.-Å., Wulff, A., 2004. Impact of Ultraviolet-B radiation on the development of phytoplankton communities in the eastern Atlantic sector of the Southern Ocean—results from on-deck model ecosystem experiments. Deep-Sea Research II, this issue [doi:10.1016/j.dsr2.2001.05.001].

Zhuang, G., Zhen, Y., Wallace, G.T., 1995. Iron(II) in rainwater, snow, and surface seawater from a coastal environment. Marine Chemistry 50, 41–50.